



Investigation of manganese oxide fouling and novel salt cleaning of an MF membrane

Chang-Ha Lee^a, Jayeong Seong^b, Joeun Lee^b, Hyung-Soo Kim^b, Sangyoup Lee^{c,*}

^aDepartment of Civil and Environmental Engineering, Sungkyunkwan University, 2066 Seobu-ro, Jangan-Gu, Suwon, Gyeonggi-do 440-746, Korea, Tel. +82-31-290-7542; Fax: +82-31-290-7549; email: ha1991@skku.edu

^bDepartment of Water Resources, Graduate School of Water Resources, Sungkyunkwan University, 2066 Seobu-ro, Jangan-Gu, Suwon, Gyeonggi-do 440-746, Korea, Tel. +82-31-290-7542; Fax: +82-31-290-7549; emails: sujayou@naver.com (J. Seong), gooaen12@naver.com (J. Lee), sookim@skku.edu (H.-S. Kim)

^cResearch Center for Environmental Technology and Policy, Korea University, 145, Anam-Ro, Seongbuk-Gu, Seoul 02841, Korea, Tel. +82-2-3290-3976; Fax: +82-2-928-7430; email: sangyoup_lee@korea.ac.kr

Received 27 August 2017; Accepted 28 October 2017

ABSTRACT

This study evaluated the cleaning efficiency of manganese and organic fouled microfiltration (MF) membranes using salt solutions. Manganese and humic acid (HA) were used as foulants separately or together. Relative permeability and filtration resistance of feed water containing only manganese and together with HA were observed. Fouling mechanisms were evaluated using the Hermia model. Flux reduction and filtration resistance increased sharply in case of feed water containing both manganese and HA. In this case, based on Hermia analysis, fouling mechanisms match well with the cake filtration and intermediate pore blocking models. By controlling the concentration of salt cleaning solutions (i.e., NaCl), flux recovery, resistance removal, foulants concentration eluted from the membrane surface and visual image of membrane surface after salt cleaning were investigated. It was clearly shown that flux recovery and resistance removal after salt cleaning increased with increasing salt concentration of cleaning solution. Notably, when using 40,000 mg/L salt cleaning solution, which is similar to seawater total dissolved solids concentration, flux recovery reached almost to the initial flux. The concentration of manganese eluted after salt cleaning also increased with increasing salt concentration of cleaning solution. In addition, membrane surface after salt cleaning is quite clear almost similar to that of clean membrane after salt cleaning. The mechanisms of salt cleaning are attributed to the osmotic swelling as well as ion-exchange. Due to osmotic swelling cake layer comprised of manganese and HA is weakened and then cross-linked manganese and HA layer is broken due to ion-exchange reaction. This study demonstrates that salt cleaning can be a useful tool for manganese fouled membrane in the presence of organic matter and the efficiency of cleaning can further optimized.

Keywords: Salt cleaning; Manganese; Fouling; Cleaning; Humic acid; Microfiltration membrane

1. Introduction

Recently, due to the deterioration in water quality and strengthened water quality standards for drinking water, the water treatment facilities are moving toward membrane filtration from the conventional filtration method, which is

the rapid sand filtration. Microfiltration (MF) and ultrafiltration (UF) technologies are increasingly used in drinking water treatment processes due to their advantages such as low energy consumption, low operating cost, simple operation and high removal efficiency of pollutants [1,2]. However, there are many adverse effects on the membrane system,

* Corresponding author.

such as flux reduction, membrane fouling, increase of trans-membrane pressure (TMP) and deterioration of membrane due to frequent cleaning [3]. Natural water contains many substances such as algae, bacteria, microorganisms, humic acid (HA) and fine particles (organic and inorganic), and they can act as submerged membrane pollutants [4]. In particular, dissolved inorganic components (e.g., manganese) were converted to solid form through oxidation, and then the oxidized particles were removed by the membrane which caused fouling on the membrane surface [5–7]. Also in the membrane filtration water treatment process, a small amount of NaOCl is injected into the treated water for physical cleaning and backwashing is performed. It is reported that manganese oxide reacts with NaOCl to deposit in the pore size of the membrane if dissolved manganese ions are present in the treated water during the backwashing [8].

It is known that manganese can degrade water quality which can have effect on taste, odor and color. It is also known that it exist in water as ions or colloids and is adsorbed on suspended particulate matter. In wetlands, manganese forms compounds with organic matter within water, such as HA [9,10]. Numerous studies have shown that the main irreversible membrane contaminants are natural organic matter in natural water containing humic substances, and when water containing HA is treated with UF, the water permeability was reduced by 30%–40% compared with the case where deionized (DI) water was used as the feed solution [11–17]. In order to reduce such fouling by manganese and HA, physical and chemical cleaning are performed. Due to the formation of manganese oxides during the physical cleaning, backwashing is necessary to prevent membrane fouling [8].

In the case of chemical cleaning, chemical cleaning agents are chosen depending on the type of contaminant. In order to remove manganese, which is an inorganic substance, acidic solution such as oxalic acid and citric acid is mainly used. To remove organic substances, strong alkaline chemicals such as NaOH and oxidizing agents such as NaOCl are generally used [18–20].

However, several studies have addressed problems such as aging of membranes caused by chemical cleaning agents and occurrence of high chemical oxygen demand (COD) cleaning effluent [21,22]. It has been demonstrated that NaOCl, a chemical agent, which is used as oxidizers can degrade membrane properties such as tensile strength, elongation and elasticity. Additionally, when organic acids such as citric acid were used for chemically enhanced backwash, the COD of the cleaning effluent was high [23].

In this study, NaCl solution was used to clean the membrane that has been fouled by HA, in order to prevent membrane aging and reduce the cleaning wastewater treatment cost.

2. Materials and methods

2.1. Membrane and raw water

The membrane used in this experiment was a polyvinylidene fluoride (PVDF) plate-type MF membrane (Durapore) with a surface area of 28.7 cm² and a pore size of 0.22 μm. Further information on membrane is listed in Table 1. Manganese used in this experiment is manganese(II) sulfate pentahydrate (MnSO₄·5H₂O, Junsei, Japan),

and sodium hypochlorite (NaOCl, 12% w/v, Showa Denko, Japan) was used as the oxidant to produce manganese oxide. As an indicator, the presence of manganese and organic matter compound, HA (Sigma-Aldrich) was used. Two different artificial feed waters, Raw-1 and Raw-2, were produced in different conditions. Raw-1 contains only manganese, and it was made by adding 435 mg of MnSO₄·5H₂O to 5 L of DI water. Raw-2 contains both manganese and HA, and it was made by adding 435 mg of MnSO₄·5H₂O and 50 mg of HA (Sigma-Aldrich) to 5 L of DI water. It is reported that the theoretical chlorine demand to oxidize manganese to manganese oxide is 1.3 mg/L of Cl₂ for 1 mg/L of Mn. [24]. However, according to the study by Choo et al. [8], when the chlorine dosage for manganese removal was increased by 3–6 times, the manganese removal efficiency was increased. Therefore, in this study, 57 mg/L of Cl₂ was injected to oxidize 19 mg/L of manganese. Table 2 shows the characteristics of feed water.

2.2. Experimental device and operation conditions

The experimental setup for this experiment is composed of a pressure vessel and a filtration device as shown in Fig. 1. For filtration device, Amicon filtration cell (Model 8200, USA) was used and it consists of membrane holder and cell body that acts as the raw water tank. For pressure vessel, the digital pressure and vessel exists in an integrated form. On the bottom of the pressure vessel, magnetic stirrer was installed in order to stir the feed solution. The permeate that passed through the membrane is set to be collected in a beaker on the digital scale that is connected to a computer for flux measurements. For filtration pressure and

Table 1
Characteristics of microfiltration membranes

Description	Microfiltration membrane
Trade name	Durapore
Filter code	GVWP09050
Pore size, μm	0.22
Filtration area, cm ²	28.7
Filter diameter, mm	63
Filter material	Polyvinylidene fluoride (PVDF)
Thickness, μm	125
Wettability	Hydrophilic
Water flow rate	>1 mL/min × cm ²

Table 2
Characteristics of feed water

Description	Raw-1 (Mn + DI water)	Raw-2 (Mn + humic + DI water)
Mn (mg/L)	19	19
TOC (mg/L)	–	9.29
pH	8.6	8.34
Temperature (°C)	22.1	22.3
Chlorine dose (mg Cl ₂ /L)	57	

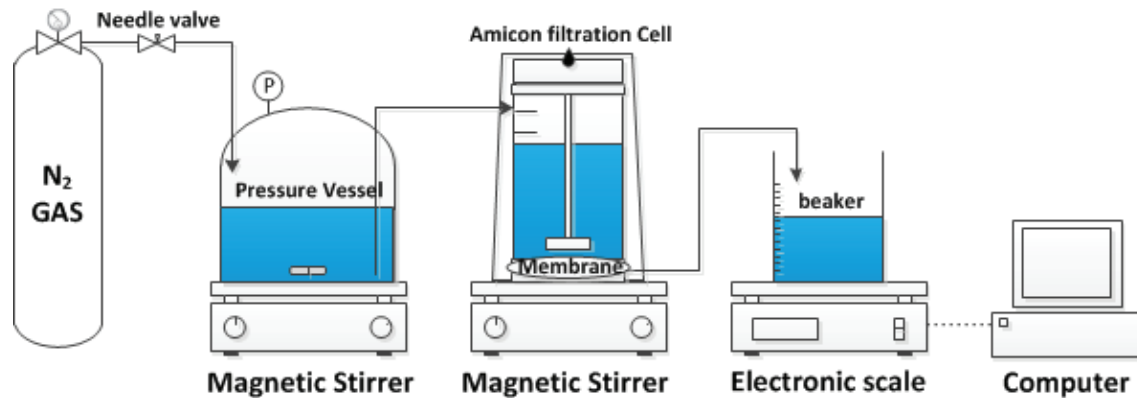


Fig. 1. Diagram of the microfiltration experimental setup.

Table 3
Amicon filtration cell operation conditions

Operation conditions	Step 1	Step 2	Step 3
Raw-1, feed water	DI water filtrated	Mn 19 mg/L + 57 mg/L as Cl ₂	DI water, NaCl 20,000 mg/L, NaCl 40,000 mg/L 2 h soaking after DI water backwash
Raw-2, feed water		Mn 19 mg/L + humic acid 10 mg/L + 57 mg/L as Cl ₂	

backwash pressure, the nitrogen gas pressure was set to 1 kg f/cm². When there are both manganese and HA present, the Amicon cell filtration process was performed in the same order as Table 3. First, using DI water, pure water flux was measured (step 1). In pressure vessel, produced artificial feed water and NaOCl was added, and flux was measured with magnetic stirrer rotating at 200 rpm, and cell body magnetic stirrer rotating at 9 rpm (step 2). Each of three identically fouled membranes was then immersed in DI water, 20,000 and 40,000 mg/L NaCl cleaning solution for 2 h. After immersing the membranes, fouled membranes were put in an opposite direction in the membrane holder, and flux was measured (step 3).

2.3. Measuring manganese elution concentration

In order to see if manganese is eluted through ion-exchange between manganese ion and sodium ion, manganese concentration in NaCl solution was measured. Similar to the method introduced in section 2.2., three membranes that are identically fouled in Raw-1 and three membranes that are identically fouled in Raw-2 were each immersed in three different solutions; DI water, 20,000 mg/L of NaCl and 40,000 mg/L of NaCl. To measure manganese elution concentration at different times, three samples were taken after 1 and 2 h, and the three values are averaged for accuracy. Cleaning conditions are listed in Table 4.

2.4. Cleaning efficiency and removal resistance

The flux (J) is calculated by the flow rate through the unit membrane area per unit time. The flux (J) through the cake and the membrane may be described by Darcy's law:

Table 4
Cleaning conditions

Description	DI water	NaCl 20,000 mg/L	NaCl 40,000 mg/L
pH	8.02	7.86	7.36
TDS (g/L)	–	20	40
Temperature (°C)	18.4	18.8	18.6
Salt contact time (h)	1, 2	1, 2	1, 2

$$J = \frac{\Delta P}{\mu R_t} \quad (1)$$

in which ΔP is TMP (driving force), μ is viscosity of the fluid and R_t is the total of the resistances. Membrane resistance (R_m) can be estimated from the initial water flux:

$$R_m = \frac{\Delta P}{\mu J_{wi}} \quad (2)$$

The resistance which appears after fouling (R_f) can be calculated from the raw water flux:

$$R_f = \left(\frac{\Delta P}{\mu J_{wf}} \right) - R_m \quad (3)$$

The resistance which remains after cleaning (R_c) can be calculated from the water flux after salt cleaning:

$$R_c = \left(\frac{\Delta P}{\mu J_{wc}} \right) - R_m \quad (4)$$

Resistance removal (RR) which is a criterion for cleaning quantification can be calculated from:

$$RR(\%) = \left[\frac{(R_f - R_c)}{R_f} \right] \times 100 \quad (5)$$

The cleaning efficiency (CE) can be calculated using Eq. (6):

$$CE(\%) = \left[\frac{(J_{wc} - J_{ww})}{(J_{wi} - J_{ww})} \right] \times 100 \quad (6)$$

Both parameters, that is, RR and CE, have been used for demonstrating the CE [25,26].

2.5. Mechanism of fouling

To determine the fouling mechanism when manganese and HA exist together, Hermia model was used. When particle size is smaller than or comparable with the membrane pores, the membrane blocking model is commonly a useful tool to explain how and when the particles penetrate into or block the pores. In the model proposed by Hermia, the relation between permeate volume and filtration time is in the form of Eq. (7) [27]:

$$\frac{d^2t}{dV^2} = k \left(\frac{dt}{dV} \right)^n \quad (7)$$

where t and V represent the filtration time and permeate volume, respectively, and k and n are parameters that has to be determined through experiments. k is the membrane surface blocked per total permeate volume, which is calculated by multiplying the mean initial velocity of the permeate. Based on the n exponent in this equation, four types of blocking mechanisms can be defined; $n = 2$ indicates complete pore blockage, $n = 1.5$ indicates pore constriction or standard blocking, $n = 1$ indicates intermediate blockage and $n = 0$ indicates cake filtration. As shown in Fig. 2, it is assumed that particles contribute in pore blockage, but do not pile on top of each other, because the particle size and pore size are the same ($d_{\text{particle}} = d_{\text{pore}}$). For standard pore blocking mechanism, particle size is much smaller than the pore size ($d_{\text{particle}} \ll d_{\text{pore}}$), thus the particles are attached on the wall of the pore, which leads to a decreased internal pore diameter. For intermediate pore blocking mechanism, it is assumed that the membrane pores are sealed due to the accumulation of particles ($d_{\text{particle}} = d_{\text{pore}}$). In cake filtration mechanism, particle size is greater than that of pore ($d_{\text{particle}} \gg d_{\text{pore}}$), causing the particles to pile on top of each other, forming a cake layer. Based on the controlling mechanism, four types of linear relationships can be established.

$$\text{Complete pore blocking: } \ln(J) = -k_{cb}t + \ln(J_0) \quad (8)$$

$$\text{Intermediate pore blocking: } J_0/J = (1 + k_i t) \quad (9)$$

$$\text{Standard pore blocking: } J_0/J = (1 + k_s t)^2 \quad (10)$$

$$\text{Cake filtration: } J_0/J = (1 + k_c t)^{1/2} \quad (11)$$

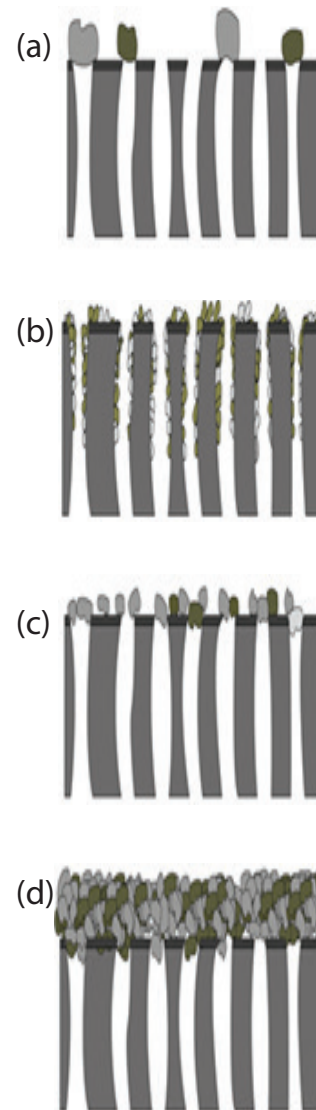


Fig. 2. Models of (a) complete blocking, (b) standard blocking, (c) intermediate blocking and (d) cake filtration.

where J_0 and J are the permeate flux per unit area through the membrane at initial and at a particular time (t), k_{cb} , k_i , k_s and k_c are blocking parameters that must be determined from the slopes of the experimental lines. Because of the intricate nature of fouling, the combination of two or three mechanisms should be considered for prediction of flux decline most of the time [28].

2.6. Analysis method

For analyses, total organic carbons (TOC), manganese ion (Mn^{2+}), total dissolved solids (TDS), pH and temperature were measured. Manganese measurement ion (Mn^{2+}) was done based on the PAN method (1-(2-pyridylazo)-2-naphthol) from Hach Company, USA. Buffer powder pillows, citrate type for manganese (Hach), sodium periodate powder pillows for manganese (Hach) was used for manganese, and the concentration of manganese was calculated by

measuring the UV absorbance at 525 nm, which was done by using Ultraviolet–visible spectrophotometer (DR6000, Hach). Three UV absorbance measurements were made in total, and the three measurements were averaged for better accuracy. For TDS and pH measurements, multimeter (HQ40d portable meter, Hach) was used.

3. Results and discussion

3.1. Evaluation of fouling by manganese oxide and the salt cleaning efficiency

3.1.1. Relative permeability and cleaning efficiency (Mn)

The fouling by manganese oxide and the effect of salt cleaning, relative permeability and CE were measured. As it can be seen in Fig. 3(a), during step 1, J/J_0 for permeating 500 mL of DI water for all three membranes were the same, having a value of 1 ± 0.05 . During step 2, 3 L of Raw-1 was filtered and J/J_0 for all three membranes was decreased. The reduction of J/J_0 for all three membranes was identical, having a value of 0.55 ± 0.02 . During step 3, after immersing the membranes in each solution for 2 h, flux was measured while backwashing was being done with DI water. For the membrane that has been back-washed with DI water, J/J_0 was 0.92, and for NaCl 20,000 and 40,000 mg/L, J/J_0 was 0.93 and 0.97, respectively. As shown in Fig. 3(b), cleaning efficiencies for the three cleaning solutions were represented with a bar graph. The cleaning efficiencies for DI water and 20,000 mg/L NaCl were 83.8% and 84%, respectively. Although higher NaCl concentration means better CE, in this case, the cleaning

efficiencies of the NaCl solution and DI water were almost the same. It seems this is due to the high manganese concentration, and due of the high manganese concentration, the high NaCl concentration, 40,000 mg/L in this case, had better CE. However, further experiments should be done to find optimal NaCl concentration for different manganese concentration.

3.1.2. Total resistance and resistance removal (Mn)

As shown in Fig. 4(a), membrane resistance when DI water was filtered (R_m) was constant, having an average value of $9.82E+10$ (step 1). After the addition of chlorine and manganese, the membrane resistance (R_f) was identically increased for all three membrane, having an average value of $1.8E+11$ (step 2). After backwashing with DI water and after cleaning with NaCl, the membrane resistance of the cleaned membrane (R_c) was $1.05E+11$ on average, which means the membrane resistance was recovered by 92.1% (step 3). Fig. 4(b) shows RR after cleaning with each cleaning solution. For DI water and 20,000 mg/L NaCl solution, the RR was 90.1% and 90.8%, respectively, having almost no difference, but for 40,000 mg/L NaCl solution, the RR was 95.3%, having a relatively higher value compared with DI water and 20,000 mg/L NaCl solution. Similar to the results from CE, cleaning was the most effective with 40,000 mg/L NaCl solution. This is because the manganese ion within the fouling layer on the membrane surface exchanges ions with sodium ions, making the fouling layer swell. The swelling of the fouling layer makes manganese oxide to attach more easily to the membrane

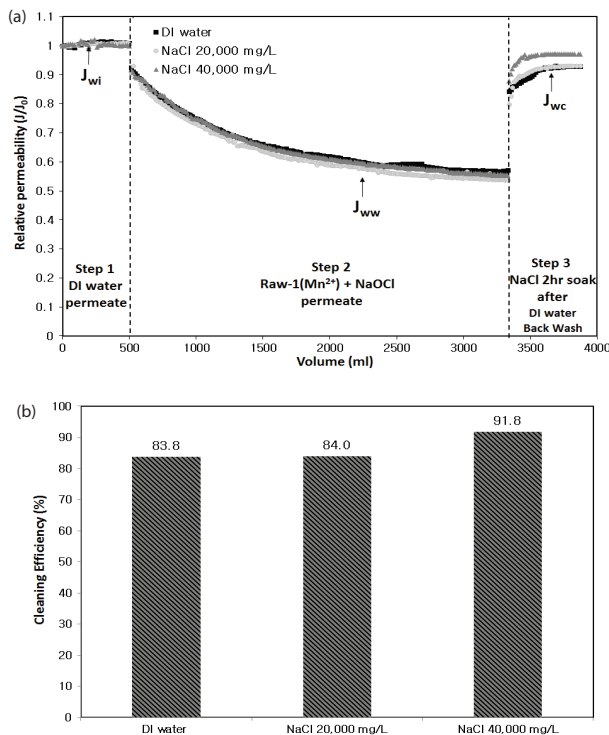


Fig. 3. Feed water (manganese oxide) (a) membrane permeability for different operating conditions and (b) salt cleaning efficiency.

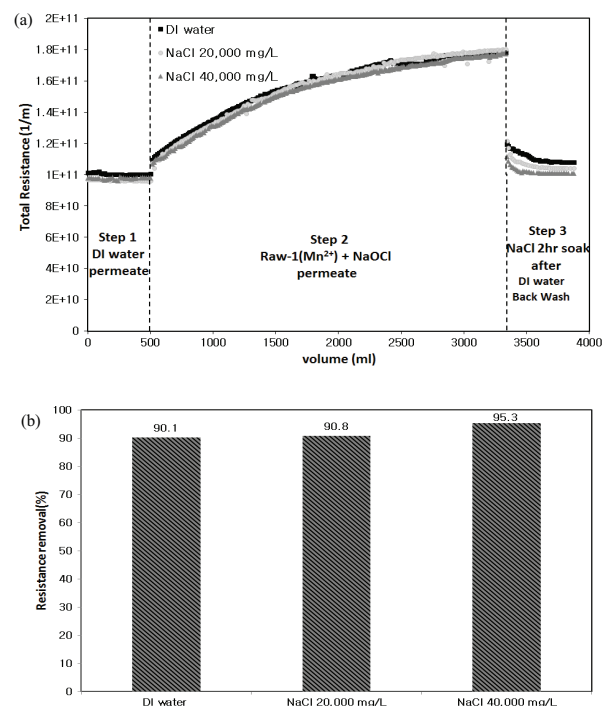


Fig. 4. Feed water (manganese oxide) (a) total filtration resistance for different operating conditions and (b) resistance removal efficiency for three cleaning solutions.

surface through the physical backwash, which results in a higher CE and thus higher resistance recovery.

3.1.3. Membrane fouling mechanism for manganese oxide

As shown in Fig. 5, in order to analyze membrane fouling mechanism due to manganese oxides, the average of three permeate flow rate values was applied in four different Hermia models. A linear relationship of $\ln(J/J_0)$ vs. t , $(J_0/J)^{0.5}$ vs. t , (J_0/J) vs. t and $(J_0/J)^2$ vs. t was determined experimentally for complete pore blocking model, standard pore blocking model, intermediate pore blocking model and cake filtration model to calculate constants (k) in models. To determine whether the data agree with any of the considered models, the coefficient of determination (R^2) of each plot for one

model was compared with the others. Therefore, continuous lines in Figs. 6–10 show deviation of curve from linear relationship [29,30]. The filtration time interval was divided from different time intervals (0–150, 0–300, 300–600, 600–1,500 and 0–1,500 s), in order to investigate how the fouling mechanism is converted during the filtration. As shown in Table 5, the cake filtration model provides the best fit to the experimental data, since its regression coefficient, R^2 is the highest.

This may be due to the formation of cake layer, which results from the piling up of manganese oxide particles that are larger than the pore size, during the entire filtration time. There are studies that have reported that the manganese oxide particles form cake layers [8].

3.1.4. Manganese elution concentration and image of membrane fouling

In this experiment, membranes were fouled with Raw-1 and Raw-2 and immersed in DI water, 20,000 mg/L NaCl solution and 40,000 mg/L NaCl solution. While the membrane is being immersed, samples were taken 1 and 2 h after the start of the immersion, and manganese in the samples were analyzed (Table 3).

As it can be seen in Fig. 11, as NaCl concentration increased, the manganese concentration also increased; however, the increase rate was not high. With 40,000 mg/L NaCl solution, compared with DI water, manganese concentration was increased by more than four times.

This result suggests that the dissolved manganese ions that are deposited on the membrane surfaces goes through ion-exchange with sodium ions. Fig. 12 also shows that the membrane surface became whiter when the concentration of NaCl is increased.

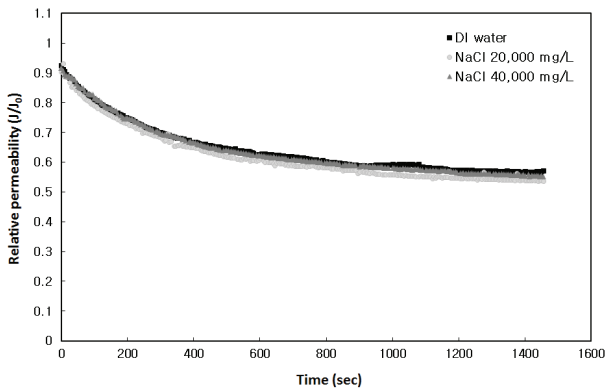


Fig. 5. Changes in relative permeability due to fouling by manganese (Mn).

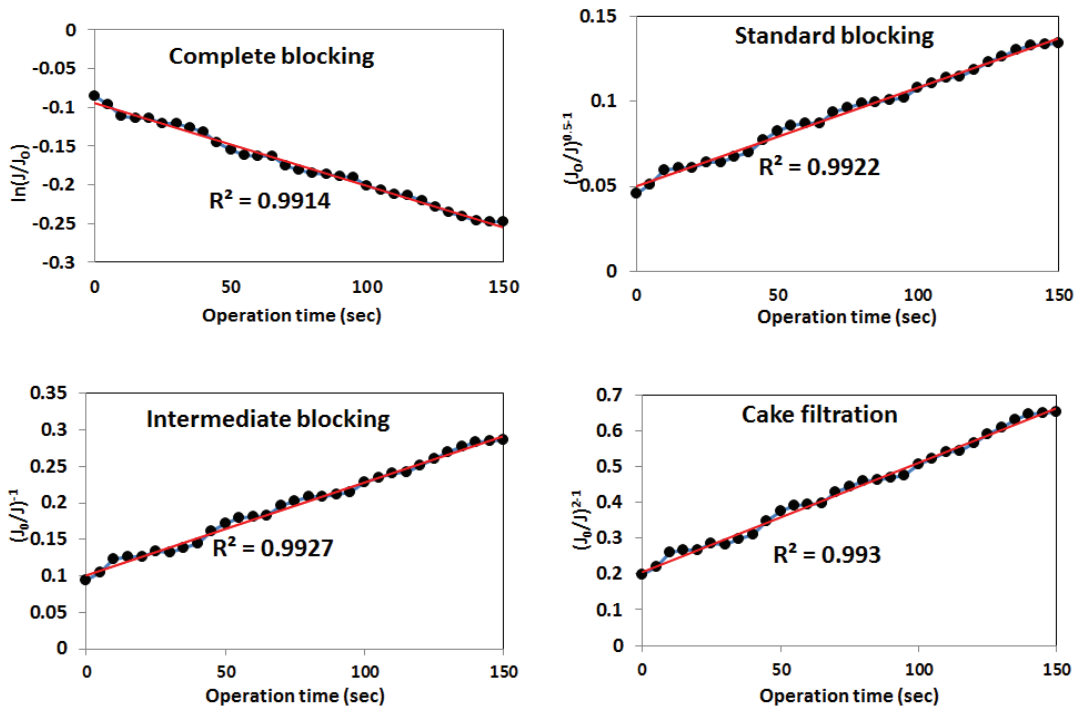


Fig. 6. Linear regression of normalized data vs. filtration time, 0–150 s (Mn).

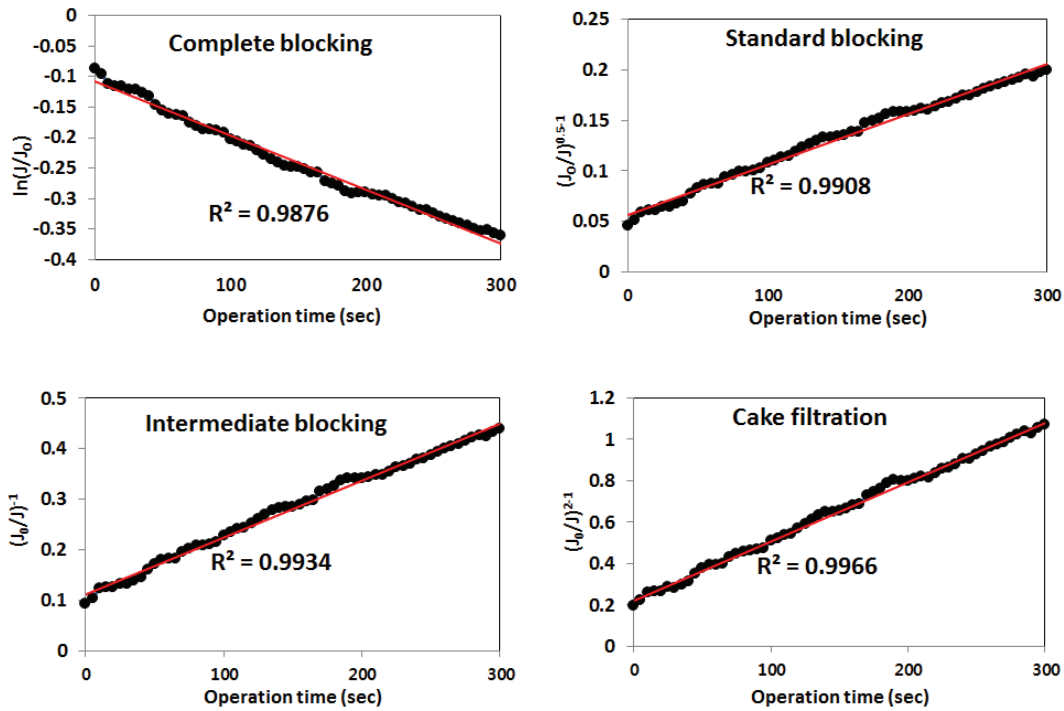


Fig. 7. Linear regression of normalized data vs. filtration time, 0–300 s (Mn).

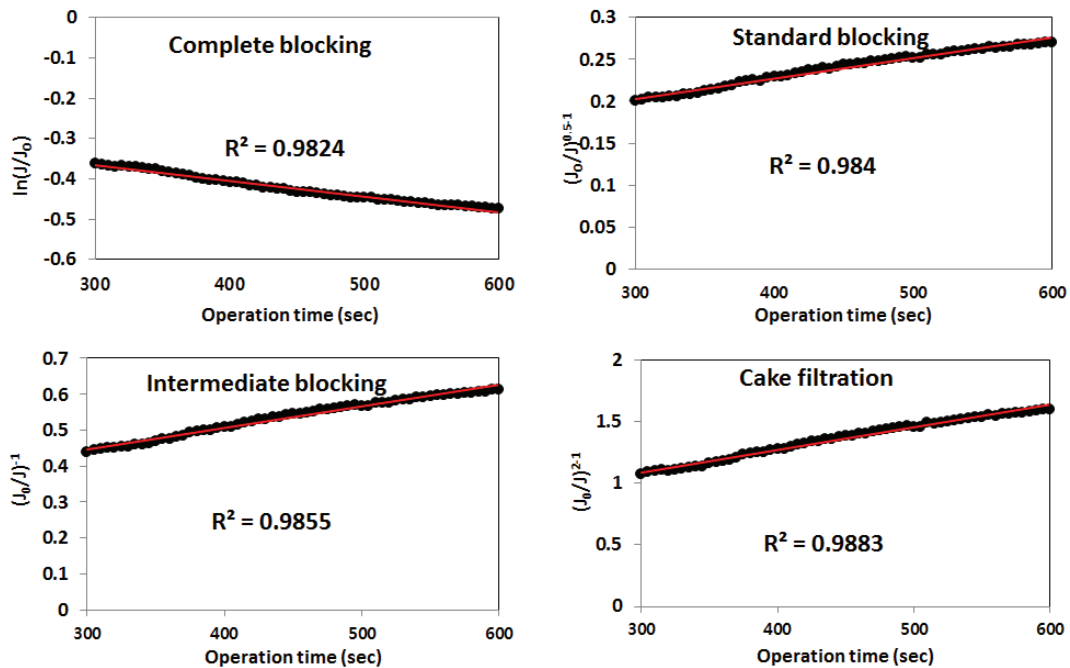


Fig. 8. Linear regression of normalized data vs. filtration time, 300–600 s (Mn).

3.2. Membrane fouling by manganese + humic acid and evaluation of salt cleaning efficiency

3.2.1. Membrane permeability and cleaning efficiency (Mn + HA)

Membrane permeability and CE were evaluated to determine the salt CE with existence of both manganese

and HA. As it can be seen in Fig. 13(a), J/J_0 for three membranes when 500 mL of DI water was being filtered, were the same, having a value of 1 ± 0.01 (step 1). When there were both HA and manganese, J/J_0 was decreased to 0.05 ± 0.01 , which is a significantly lower value than that of the case where there is only manganese present (step 2). According to previous studies' results, this is because HAs

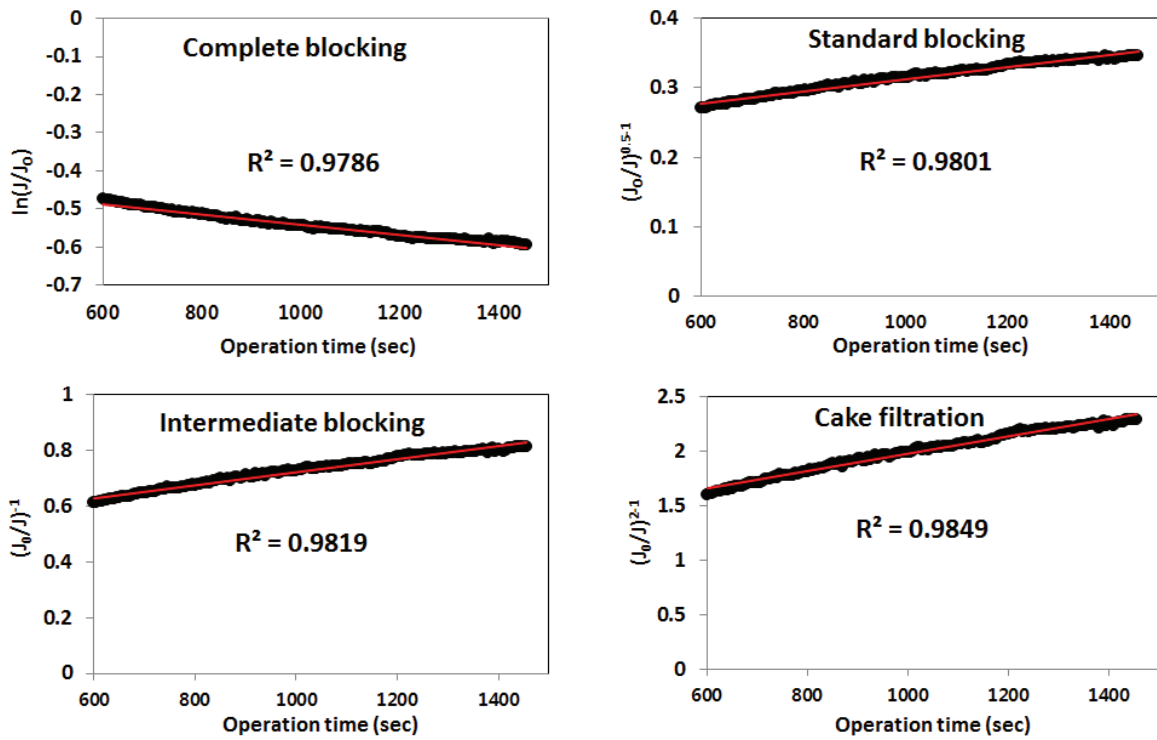


Fig. 9. Linear regression of normalized data vs. filtration time, 600–1,500 s (Mn).

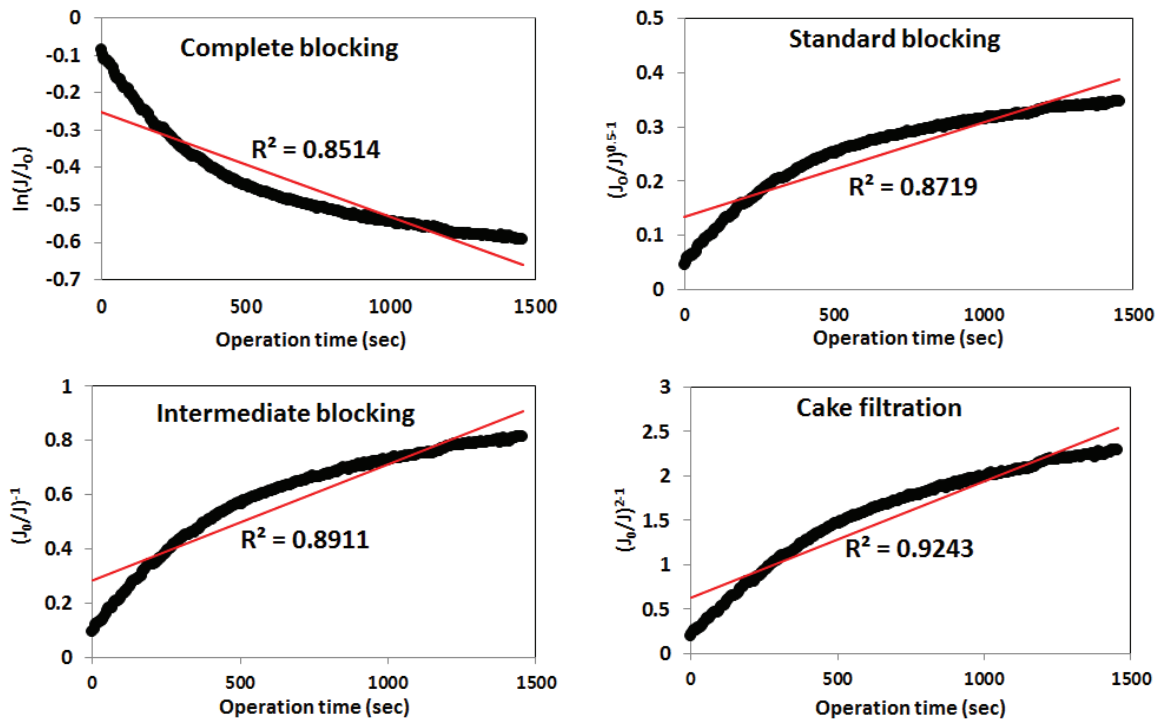


Fig. 10. Linear regression of normalized data vs. filtration time, 0–1,500 s (Mn).

have characteristic of forming a strong chelate with divalent ions, causing a severe fouling [31]. During step 3, flux was measured while performing a backwash with DI water after immersing the membrane for 2 h in each cleaning solution.

The membrane that was cleaned with DI water had J/J_0 value of 0.54, and for 20,000 and 40,000 mg/L of NaCl solution, the J/J_0 values were 0.60 and 0.76, respectively. As shown in Fig. 13(b), the cleaning efficiencies were measured

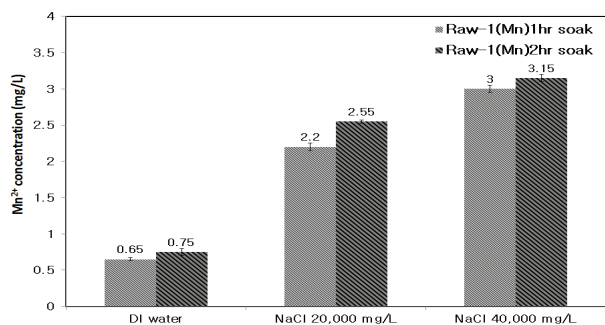
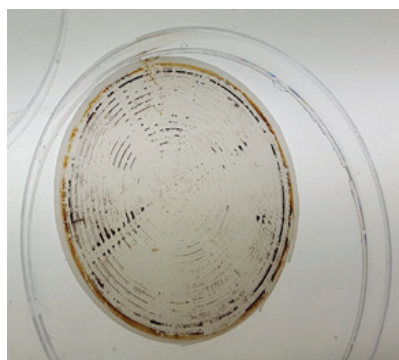


Fig. 11. Manganese elution concentration for each cleaning solution at 1 and 2 h soaking time.



DI water



NaCl 20,000 mg/L



NaCl 40,000 mg/L

Fig. 12. Image of fouled membrane after cleaning (Mn).

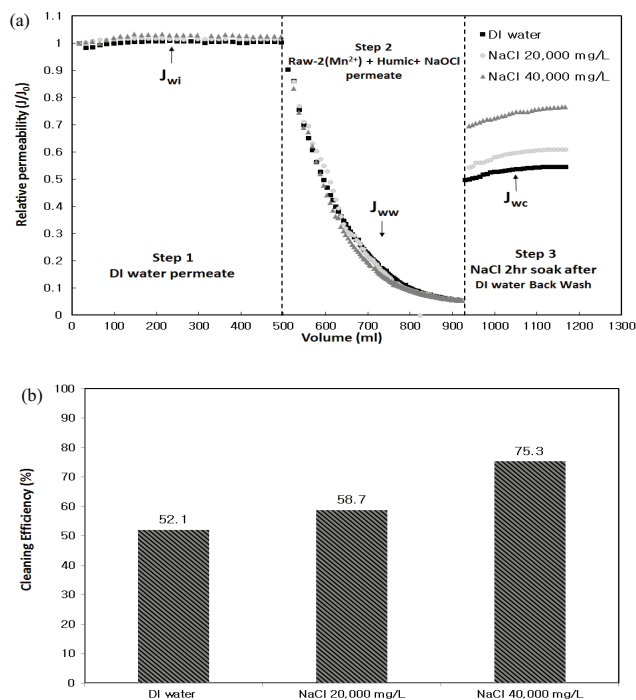


Fig. 13. Feed water (manganese oxide + HA) (a) membrane permeability for different operating conditions and (b) cleaning efficiency of three cleaning solutions.

to be 58.7% and 75.3% for 20,000 and 40,000 mg/L of NaCl solution, respectively, and for DI water, the CE was 52.1%. Similar to the case without HA, there was no big difference in CE for DI water and 20,000 mg/L NaCl, which is around 6%, however, for 40,000 mg/L NaCl, the cleaning was around 20%, which is significantly higher than the DI water and 20,000 mg/L NaCl.

3.2.2. Total resistance and resistance removal efficiency (Mn + HA)

When DI water was being filtered, the membrane resistance (R_m) had a consistent value of $9.32E+10$, and this can be seen in Fig. 14(a) (step 1). The fouling resistance, which was measured after injecting chlorine into solution containing both manganese and HA, was measured to have an average value of $1.76E+12$. This great increase in resistance indicates a rapid and severe fouling. Cleaned membrane filtration resistance (R_c) was measured to be $1.69E+11$ when the membrane was cleaned with DI water, $1.56E+11$ and $1.21E+11$, after salt cleaning with 20,000 and 40,000 mg/L of NaCl solution, respectively. Compared with DI water, NaCl solutions had more impact on reducing the resistance, and as the salt concentration increased, there was greater reduction in resistance. Fig. 14(b) shows the RR. From the results, DI water and 20,000 mg/L NaCl solution showed similar RR, having values of 95.4% and 96.3%, respectively. However, for 40,000 mg/L NaCl solution, the RR was 98.3%, having a relatively high removal compared with those of DI water and 20,000 mg/L NaCl solution. Similar to the results from previous experiment,

40,000 mg/L NaCl solution has shown the greatest performance in removing the resistance.

3.2.3. Mechanism of fouling resulting from the bonding between manganese and humic acid

To analyze the mechanism for fouling that results from the bonding between manganese oxides and HAs,

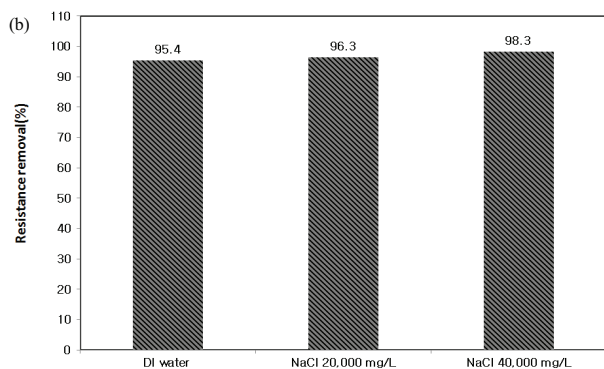
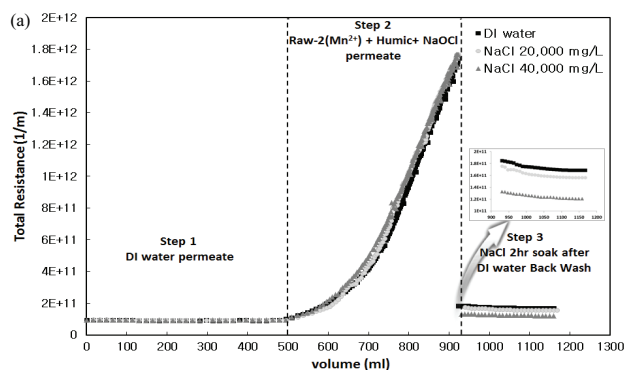


Fig. 14. Feed water (manganese oxide + HA) (a) total filtration resistance for different operating conditions and (b) resistance removal efficiency for three different cleaning solution.

three permeate flow rate values taken over time was averaged, and the average value was applied to Hermia model, as shown in Fig. 15. In order to determine the model that matches with the experimental data, R^2 value was compared with the values in Table 6. Additionally, Figs. 16–20 show the deviation of the curve from the linear relationship. Also, how the fouling mechanism switches was investigated for different time intervals (0–150, 0–300, 300–600, 600–900 and 0–900 s). It was found that during the initial filtration time, 0–150 and 0–300 s, the R^2 value of intermediate pore blocking model has the highest value. Similar to the flux reduction experiment, during the early stage of filtration, manganese and HA compound particles accumulated on the membrane surface, blocking the pores that lead to drastic reduction in flux. From the results, it can be seen that during the mid- and late-stage, which is 300–600 and 600–900 s, respectively, the main mechanism is cake filtration model and the R^2 value is the highest. It seems that this is because during the mid- and late-stage, the particles piled up after the pore blockage during the early stage, which lead to a formation of cake layer.

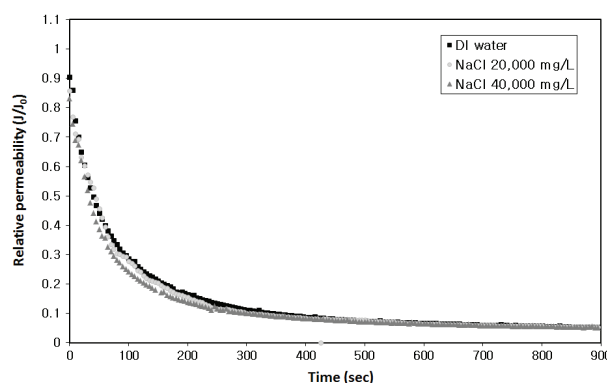


Fig. 15. Changes in relative permeability after fouling on the membrane (Mn + HA).

Table 5
Comparison of R^2 values at different time interval for fouling prediction (Mn)

Mechanism	0–150 (s)	0–300 (s)	300–600 (s)	600–1,500 (s)	0–1,500 (s)
Complete blocking	0.9914	0.9876	0.9824	0.9786	0.8514
Standard blocking	0.9922	0.9908	0.9840	0.9801	0.8719
Intermediate blocking	0.9927	0.9934	0.9855	0.9819	0.8911
Cake filtration	0.9930	0.9966	0.9883	0.9849	0.9243

Table 6
Comparison of R^2 values for predicting fouling behavior at different filtration time interval (Mn + HA)

Mechanism	0–150 (s)	0–300 (s)	300–600 (s)	600–900 (s)	0–900 (s)
Complete blocking	0.9717	0.9452	0.9866	0.9905	0.8062
Standard blocking	0.9938	0.9895	0.9923	0.9917	0.9126
Intermediate blocking	0.9984	0.9984	0.9960	0.9925	0.9716
Cake filtration	0.9651	0.9472	0.9971	0.9929	0.9946

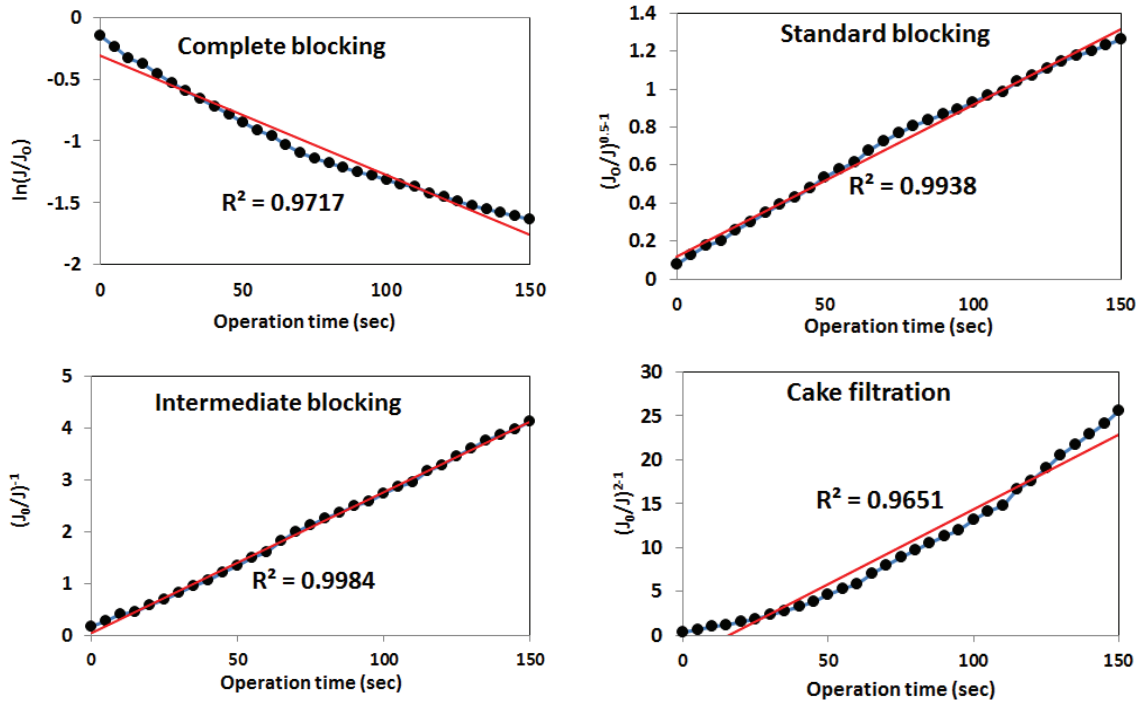


Fig. 16. Linear regression of normalized data vs. filtration time, 0–150 s (Mn + HA).

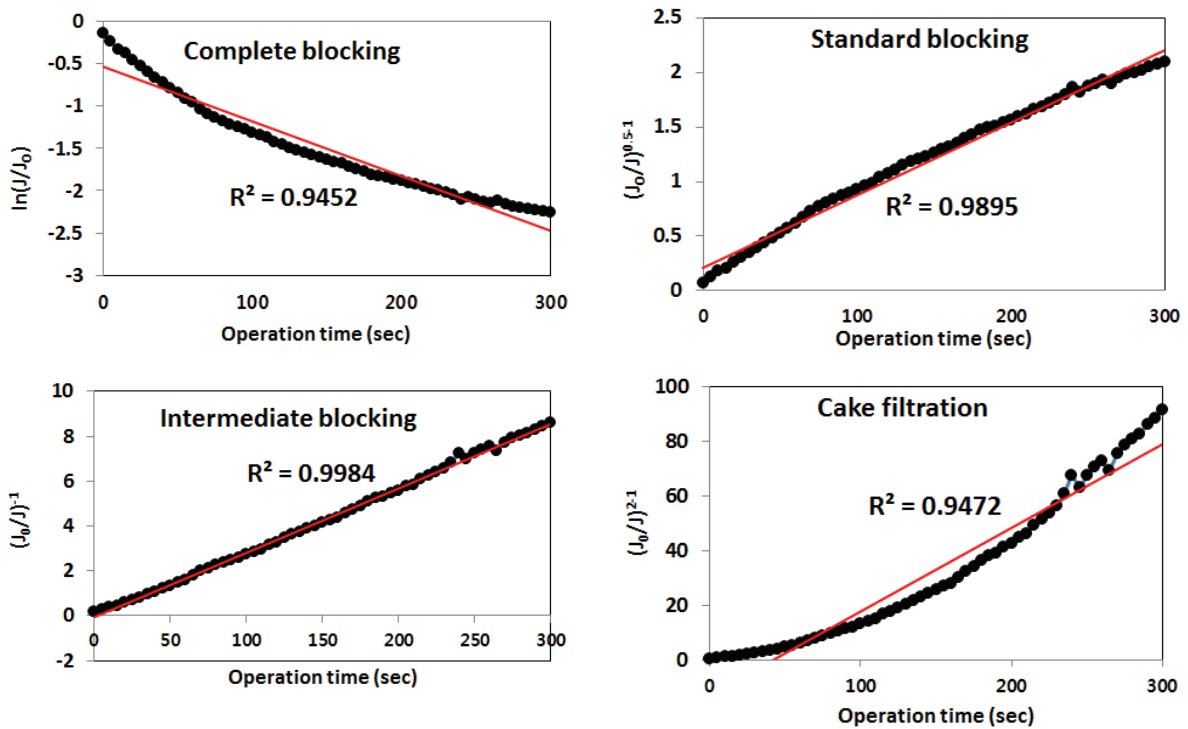


Fig. 17. Linear regression of normalized data vs. filtration time, 0–300 s (Mn + HA).

3.2.4. Manganese elution concentration and image of membrane fouling (Mn + HA)

In this experiment, as shown in Table 3, membranes that are fouled by Raw-2 and step 2 condition were each

immersed in DI water, 20,000 and 40,000 mg/L NaCl solution and samples were taken every hour for 2 h to analyze manganese within the samples. Similar to the case where there is only manganese present, as NaCl concentration increased,

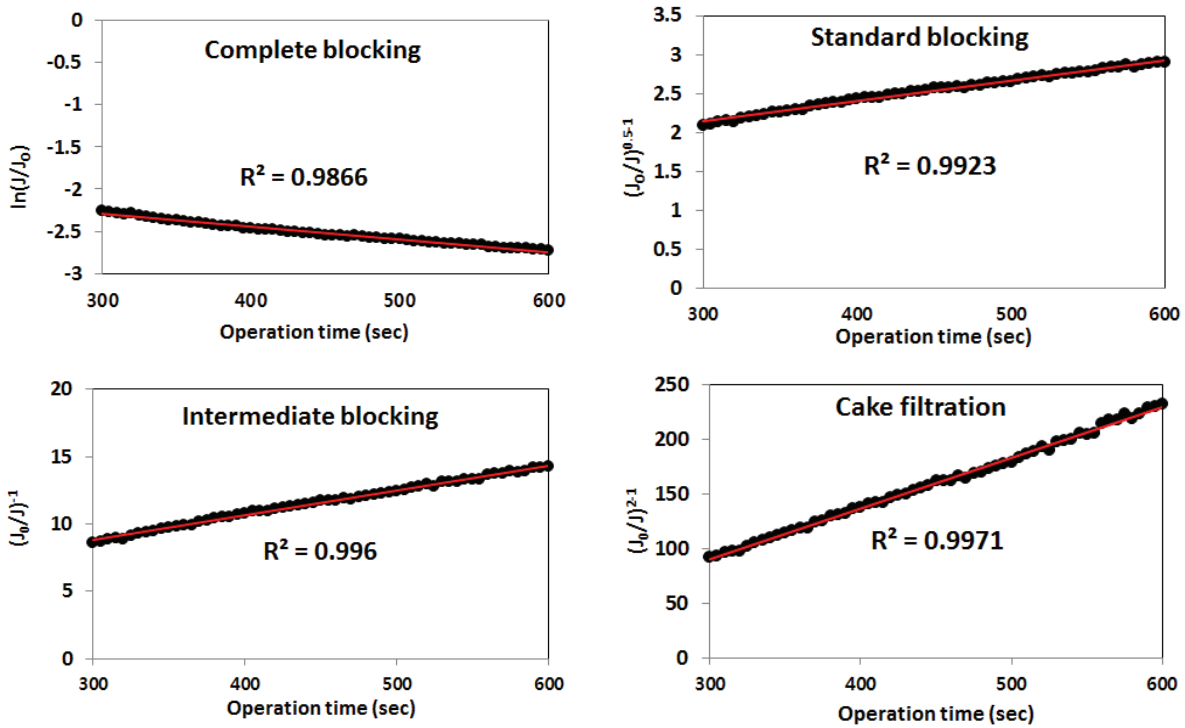


Fig. 18. Linear regression of normalized data vs. filtration time, 300–600 s (Mn + HA).

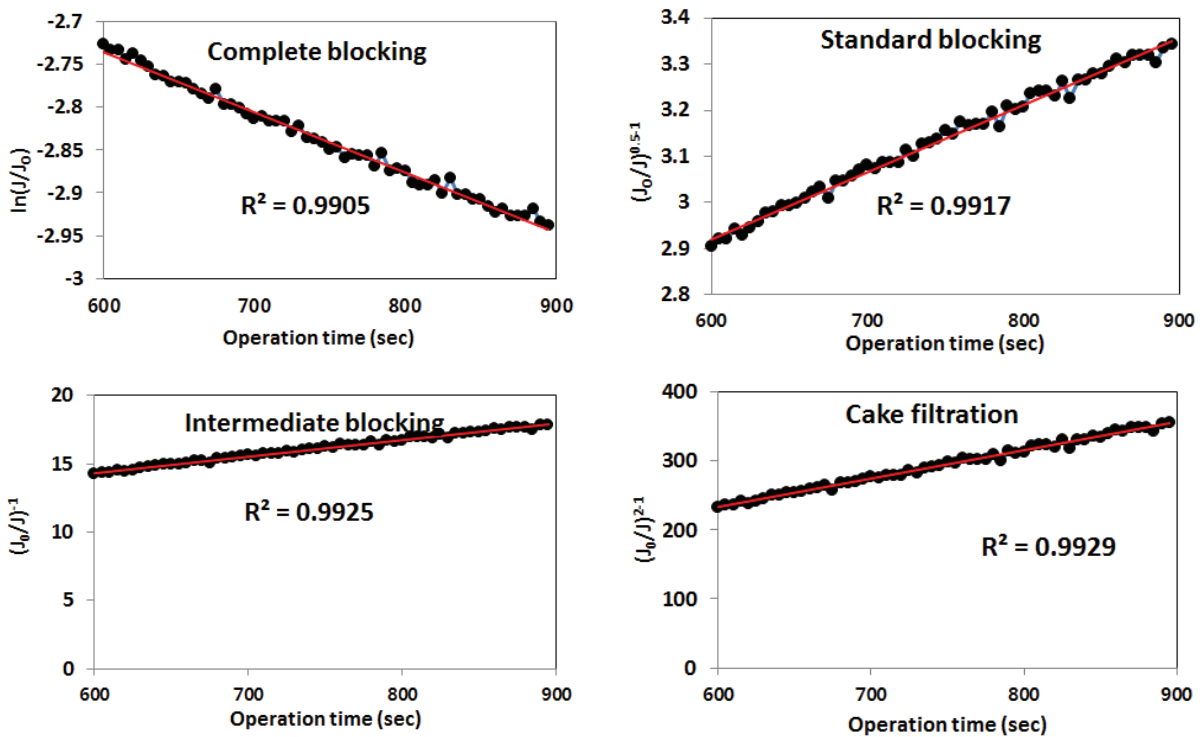


Fig. 19. Linear regression of normalized data vs. filtration time, 600–900 s (Mn + HA).

the manganese concentration increased, but the increase rate was not affected by time and this can be seen in Fig. 21. With 40,000 mg/L solution the manganese concentration

increased more than 3.5 times compared with DI water. As mentioned earlier, it seems the manganese is eluted due to the ion-exchange and swelling of the cake layer after the salt

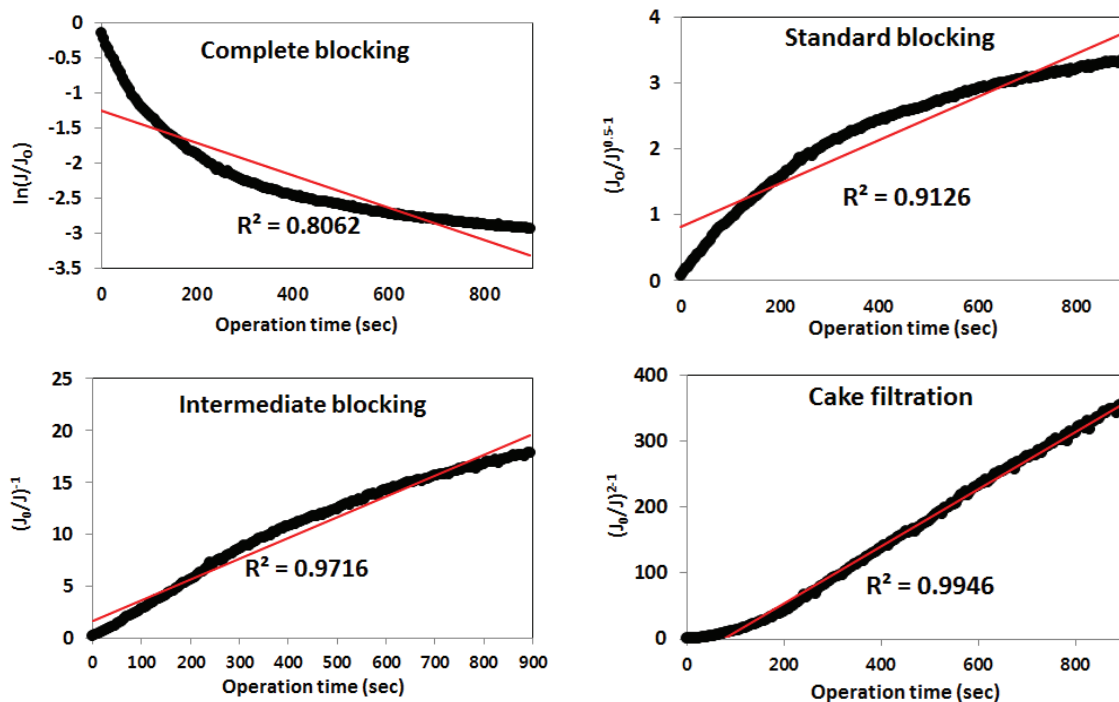


Fig. 20. Linear regression of normalized data vs. filtration time, 0–900 s (Mn + HA).

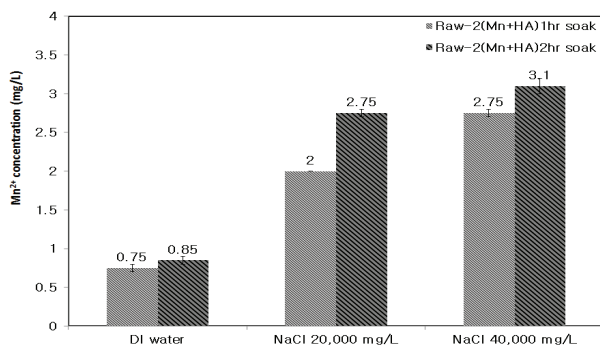


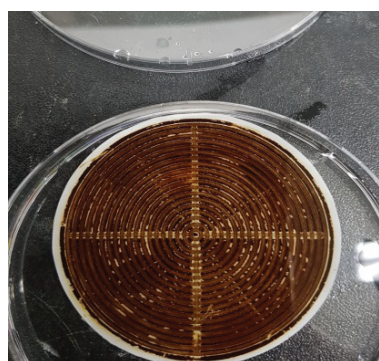
Fig. 21. Manganese elution concentration for each cleaning solution at 1 and 2 h soaking time (Mn + HA).

cleaning. According to Lee and Elimelech [32], divalent cations form bonds with organic matters, forming a gel layer, and when the salt cleaning is performed, the gel network breaks down due to the change in structure and the ion-exchange. After the experiment, as shown in Fig. 22, it was observed that the membrane surface became whiter with increasing concentration of NaCl.

4. Conclusions

In this study, membrane CE and membrane fouling mechanisms were compared and evaluated by applying salt cleaning, for controlling the fouling by manganese oxide and HA in membrane filtration process. In comparison with manganese, when the feed water contained both manganese and HA, there was a rapid flux reduction. Also, according to the analysis of the fouling mechanism, early

stage indicated intermediate pore blocking and mid- and late-stage indicated cake filtration model. It was found that this is because the particle formed by manganese and humic blocks the pores, reducing the flux, and piling up of those particles results in a cake layer in mid- and late-stage. Also, for feed water containing only manganese, membrane fouling due to cake layer during the entire filtration time was observed. As it can be seen, the membrane that was fouled by both manganese and HA resulted in higher elution concentration of manganese after immersing in salt solution, compared with the DI water, which is due to the ion-exchange between the cake layer and the salt ion. Also, the RR efficiency and the CE were the highest for NaCl concentration of 40,000 mg/L. Also, the effect of salt cleaning was small when there was HA present; however, there was a great difference depending on the salt concentration. This is because manganese ions bond with HAs, forming a cake layer on the membrane surface, and by cleaning with salt solution, the sodium ion and cations exchange ions, making the structure looser, hence the greater dependence on salt concentration. Since there was not much difference in CE for DI water and 20,000 mg/L of NaCl solution, it seems more studies should be conducted to find optimal salt concentration for each manganese concentration, in order to increase CE. Through the results from this study, salt cleaning is effective in controlling the fouling by manganese oxide and HA. In future studies, it is necessary to compare the cleaning effect for feed water with just HA and feed water with both manganese oxide with HA. At currently operating 30,000 m³/d G membrane filtration plant, it costs about 50 million won/year to dispose the chemical cleaning agents and the waste solution, and there is a deterioration in membrane due to chemical cleaning. Therefore,



DI water



NaCl 20,000 mg/L



NaCl 40,000 mg/L

Fig. 22. Image of fouled membrane after cleaning (Mn + HA).

it is believed that by using salt cleaning, the cost of disposing the chemicals and waste solutions will be reduced as well as the cost of the membrane replacement due to the deterioration.

Acknowledgments

This research was supported by Korea Ministry of Environment as “Global Top Project (2016002100001)”. This research was supported by a grant (code 171FIP-C088924-04) from Industrial Facilities & Infrastructure Research Program funded by Ministry of Land, Infrastructure and

Transport (MOLIT) of the Korea government and the Korea Agency for Infrastructure Technology Advancement (KAIA).

Symbols

J	—	Permeation flux through membrane, $\text{m}^3/\text{m}^2 \text{ s}$
J_{wi}	—	Membrane permeation flux, $\text{m}^3/\text{m}^2 \text{ s}$
J_{wv}	—	Fouled membrane permeation flux, $\text{m}^3/\text{m}^2 \text{ s}$
J_{wc}	—	Cleaned membrane permeation flux, $\text{m}^3/\text{m}^2 \text{ s}$
R_t	—	Total filtration resistance, m^{-1}
R_m	—	Membrane resistance, m^{-1}
R_f	—	Fouled membrane resistance, m^{-1}
R_c	—	Cleaned membrane resistance, m^{-1}
ΔP	—	Transmembrane pressure, Pa
μ	—	Viscosity, Pa s
RR	—	Resistance removal, %
CE	—	Cleaning efficiency, %

References

- [1] G.S. Ajmani, D. Goodwin, K. Marsh, D.H. Fairbrother, K.J. Schwab, J.G. Jacangelo, H. Huang, Modification of low pressure membranes with carbon nanotube layers for fouling control, *Water Res.*, 46 (2012) 5645–5654.
- [2] M. Laine, C. Campos, I. Baudin, L. Janex, Understanding membrane fouling: a review of over a decade of research, *Water Sci. Technol. Water Supply*, 3 (2003) 155–164.
- [3] T.A. Kurniawan, G.Y.S. Chan, W. Lo, S. Babel, Physico-chemical treatment techniques for wastewater laden with heavy metals, *Chem. Eng. J.*, 118 (2006) 83–98.
- [4] M. Kabsch-Korbutowicz, K. Majewska-Nowak, T. Winnicki, Analysis of membrane fouling in the treatment of water solutions containing humic acids and mineral salts, *Desalination*, 126 (1999) 179–185.
- [5] Y. Kaiya, Y. Itoh, K. Fujita, S. Takizawa, Study on fouling materials in the membrane treatment process for potable water, *Desalination*, 106 (1996) 71–77.
- [6] D.A. Reckhow, W.R. Knocke, M.J. Kearney, C.A. Parks, Oxidation of iron and manganese by ozone, *Ozone Sci. Eng.*, 13 (1991) 675–695.
- [7] J. Sallanko, E. Lakso, M. Lehmikangas, The effect of ozonation on the size fractions of manganese, *Ozone Sci. Eng.*, 27 (2005) 147–151.
- [8] K. Choo, H. Lee, S. Choi, Iron and manganese removal and membrane fouling during UF in conjunction with prechlorination for drinking water treatment, *J. Membr. Sci.*, 267 (2005) 18–26.
- [9] T. Suzuki, Y. Watanabe, G. Ozawa, S. Ikeda, Removal of soluble organics and manganese by a hybrid MF hollow fiber membrane system, *Desalination*, 117 (1998) 119–129.
- [10] World Health Organization, *Guidelines for Drinking Water Quality*, 3rd ed., WHO, 2008, 668 p.
- [11] M. Nyström, K. Ruohomäki, L. Kaipia, Humic acid as a fouling agent in filtration, *Desalination*, 106 (1996) 79–87.
- [12] T. Carroll, S. King, S.R. Gray, B.A. Bolto, N.A. Booker, The fouling of microfiltration membrane by NOM after coagulation treatment, *Water Res.*, 34 (2002) 2861–2868.
- [13] J. Haberkamp, M. Ernst, G. Makdissy, P.M. Huck, M. Jekel, Protein fouling of ultrafiltration membranes — investigation of several factors relevant for tertiary wastewater treatment, *J. Environ. Eng. Sci.*, 7 (2008) 651–660.
- [14] K.S. Katsoufidou, D.C. Sioutopoulos, S.G. Yiantsios, A.J. Karabelas, UF membrane fouling by mixtures of humic acids and sodium alginate: fouling mechanisms and reversibility, *Desalination*, 264 (2010) 220–227.
- [15] J. Tian, M. Ernst, F. Cui, M. Jekel, Correlations of relevant membrane foulants with UF membrane fouling in different waters, *Water Res.*, 47 (2013) 1218–1228.

- [16] W. Sun, J. Nan, J. Xing, J. Tian, Influence and mechanism of different molecular weight organic molecules in natural water on ultrafiltration membrane fouling reversibility, *J. R. Soc. Chem.*, 6 (2016) 83456–83465.
- [17] K. Majewska-Nowak, M. Kabsch-Korbutowicz, T. Winnicki, Capillary membranes for separation of dye particles, *Desalination*, 105 (1996) 91–103.
- [18] F.S. Thomas, R.S. Summers, M.G. Alison, Nanofiltration foulants from treated surface water, *Environ. Sci. Technol.*, 32 (1998) 3612–3617.
- [19] Y.-C. Su, J.-C. Wu, C.-H. Lin, Analysis of UF Membranes at the Industrial Wastewater Purification Plant at China Steel, *China Steel Technical Report*, Vol. 29, 2016, pp. 37–43.
- [20] N. Porcelli, S. Judd, Chemical cleaning of potable water membranes: a review, *Sep. Purif. Technol.*, 71 (2010) 137–143.
- [21] E. Arkhangelsky, D. Kuzmenko, N.V. Gitis, M. Vinogradov, S. Kuiry, V. Gitis, Hypochlorite cleaning causes degradation of polymer membranes, *Tribol. Lett.*, 28 (2007) 109–116.
- [22] Y. He, J. Sharma, R. Bogati, B.Q. Liao, C. Goodwin, K. Marshall, Impacts of aging and chemical cleaning on the properties and performance of ultrafiltration membranes in potable water treatment, *Sep. Sci. Technol.*, 49 (2014) 1317–1325.
- [23] S.L. Clemens, W.C. Faulkner, E.B. Browning, J.S. Murray, L.M. Alcott, H.B. Stowe, C.A. Sandburg, The effect of ocean acidification on calcifying organisms in marine ecosystems: an organism-to-ecosystem perspective, *Annu. Rev. Ecol. Evol. Syst.*, 41 (2010) 127–147.
- [24] J.K. Kim, S.G. Jeong, J.S. Kim, S.J. Park, Manganese removal in water treatment processes, *J. Korean Soc. Water Wastewater*, 19 (2005) 595–604.
- [25] M. Bartlett, M.R. Bird, J.A. Howell, An experimental study for the development of a qualitative membrane cleaning model, *J. Membr. Sci.*, 105 (1995) 147–157.
- [26] C. Liu, S. Caothien, J. Hayes, T. Caothuy, Membrane Chemical Cleaning: From Art to Science, *Proc. AWWA 2000 Water Quality Technology Conference*, Denver, CO, 2001.
- [27] J. Hermia, Constant pressure blocking filtration law: application to power law non-Newtonian fluids, *Trans. Inst. Chem. Eng.*, 60 (1982) 183–187.
- [28] C. Duclos-Orsello, W. Li, C. Ho, A three mechanism model to describe fouling of microfiltration membranes, *J. Membr. Sci.*, 280 (2006) 856–866.
- [29] M. Abbasi, D. Mowla, Analysis of membrane pore-blocking models applied to the MF of real oily wastewaters treatment using mullite and mullite–alumina ceramic membranes, *Desal. Wat. Treat.*, 52 (2014) 2481–2493.
- [30] H. Esfahani, M.P. Prabhakaran, E. Salahi, A. Tayebifard, M.R. Rahimpour, M. Keyanpour-Rad, S. Ramakrishna, Electrospun nylon 6/zinc doped hydroxyapatite membrane for protein separation: mechanism of fouling and blocking model, *Mater. Sci. Eng., C*, 59 (2016) 420–428.
- [31] C. Jucker, M.M. Clark, Adsorption of aquatic humic substances on hydrophobic ultrafiltration membranes, *J. Membr. Sci.*, 97 (1994) 37–52.
- [32] S. Lee, M. Elimelech, Salt cleaning of organic-fouled reverse osmosis membranes, *Water Res.*, 41 (2007) 1134–1142.